New Phytologist

Research

FGB1 and WSC3 are *in planta*-induced β-glucan-binding fungal lectins with different functions

Stephan Wawra[1]*, Philipp Fesel[1]*, Heidi Widmer[1], Ulla Neumann[2], Urs Lahrmann[1], Stefan Becker[3,4], Jan-Hendrik Hehemann[3,4], Gregor Langen[1] and Alga Zuccaro[1]

[1]Botanical Institute, Cluster of Excellence on Plant Sciences (CEPLAS), Cologne Biocenter, University of Cologne, Cologne 50674, Germany; [2]Central Microscopy (CeMic), Max Planck Institute for Plant Breeding Research, Cologne 50829, Germany; [3]Max Planck Institute for Marine Microbiology, Bremen 28359, Germany; [4]Center for Marine Environmental Sciences, University of Bremen, MARUM, Bremen 28359, Germany

Author for correspondence:
Alga Zuccaro
Tel: +49 221 470 7170
Email: azuccaro@uni-koeln.de

Received: *11 December 2018*
Accepted: *12 January 2019*

New Phytologist (2019) **222:** 1493–1506
doi: 10.1111/nph.15711

Key words: *Bipolaris sorokiniana*, carbohydrate-binding lectin, cell-wall-integrity-and-stress-response-component, *Colletotrichum tofieldiae*, glucan-matrix, isothermal titration calorimetry (ITC), microscale thermophoresis.

Summary

- In the root endophyte *Serendipita indica*, several lectin-like members of the expanded multigene family of WSC proteins are transcriptionally induced *in planta* and are potentially involved in β-glucan remodeling at the fungal cell wall.
- Using biochemical and cytological approaches we show that one of these lectins, *Si*WSC3 with three WSC domains, is an integral fungal cell wall component that binds to long-chain β1-3-glucan but has no affinity for shorter β1-3- or β1-6-linked glucose oligomers. Comparative analysis with the previously identified β-glucan-binding lectin *Si*FGB1 demonstrated that whereas *Si*WSC3 does not require β1-6-linked glucose for efficient binding to branched β1-3-glucan, *Si*FGB1 does.
- In contrast to *Si*FGB1, the multivalent *Si*WSC3 lectin can efficiently agglutinate fungal cells and is additionally induced during fungus–fungus confrontation, suggesting different functions for these two β-glucan-binding lectins.
- Our results highlight the importance of the β-glucan cell wall component in plant–fungus interactions and the potential of β-glucan-binding lectins as specific detection tools for fungi *in vivo*.

Introduction

Plant root-associated fungi thrive in challenging and rapidly changing environments. Their ability to colonize their hosts depends, among others, on their capacity to remodel the cell surface to withstand biotic and abiotic stresses and to limit plant immune recognition. The fungal cell wall (CW) is the first cellular structure that is exposed to the plant host and to other microbes. CW-derived polysaccharides, such as chitin and β-glucans, are potent elicitors of plant immune responses and thus their detection needs to be prevented while maintaining CW integrity for successful colonization (Rovenich *et al.*, 2016; Geoghegan *et al.*, 2017; Latge *et al.*, 2017; Hopke *et al.*, 2018). Additionally, CW integrity plays a role in the response to other microbes in the soil. To avoid recognition of CW-derived polysaccharides and to limit stimulation of plant defense responses, fungi have evolved different strategies such as CW remodeling, masking, shielding and manipulation of glycan-induced host defense signaling (El Gueddari *et al.*, 2002; van den Burg *et al.*, 2006; de Jonge *et al.*, 2010; Marshall *et al.*, 2011; Fujikawa *et al.*, 2012; Mentlak *et al.*, 2012; Oliveira-Garcia & Deising, 2013, 2016; Sanchez-Vallet *et al.*, 2013; Fesel & Zuccaro, 2016a; Takahara *et al.*, 2016; Wawra *et al.*, 2016; Melida *et al.*, 2018). Whereas several mechanisms of chitin masking/shielding and avoidance of plant host immune perception are known, fungal mechanisms dedicated to the modulation of β-glucan recognition have only been described recently (Emsley & Cowtan, 2004; Oliveira-Garcia & Deising, 2013, 2016; Wawra *et al.*, 2016). In the maize (*Zea mays*) pathogen *Colletotrichum graminicola*, synthesis of β-glucan is rigorously downregulated during biotrophic development in the plant host possibly leading to a depletion of this polymer at the CW of biotrophic hyphae (Oliveira-Garcia & Deising, 2016). A further strategy for evading β-glucan-triggered immunity is given by the fungal specific β-glucan-binding lectin FGB1 of the root endophyte *Serendipita indica* (*Si*, syn. *Piriformospora indica*). *Si*FGB1 was shown to bind β-glucan with high specificity and to be capable of suppressing β-glucan-triggered immunity in different plants (Wawra *et al.*, 2016).

Sequencing of several genomes from root-associated fungi uncovered an expansion in the sebacinoid genomes of genes encoding proteins with carbohydrate-binding properties (Zuccaro *et al.*, 2011; Lahrmann & Zuccaro, 2012; Kohler *et al.*, 2015). The physiological relevance of this expansion is unclear but a large set of these genes are transcriptionally induced during root colonization of different hosts suggesting that they

*These authors contributed equally to this work.

contribute to the endophytic lifestyle of these fungi (Zuccaro *et al.*, 2011; Lahrmann & Zuccaro, 2012; Kohler *et al.*, 2015; Lahrmann *et al.*, 2015; Fesel & Zuccaro, 2016b). Specifically, genes encoding lectin-like proteins such as the chitin-binding LysM (Lysin Motif) proteins which are known as suppressors of host immunity, the cellulose-binding CBM1 (Carbohydrate-Binding Module Family 1) proteins, which are potentially involved in loosening of the plant CW, and proteins with WSC domain(s) (cell wall integrity and stress response components) are remarkably enriched (Gaulin *et al.*, 2002; Saloheimo *et al.*, 2002; de Jonge & Thomma, 2009; Lahrmann & Zuccaro, 2012; Kohler *et al.*, 2015). The *S. indica* genome encodes for 36 WSC proteins with 23 of those being significantly differentially expressed during colonization of plant roots (Zuccaro *et al.*, 2011; Lahrmann & Zuccaro, 2012). Twenty-eight of the WSC domain-containing proteins are predicted to be lectins devoid of known enzymatic domains (Goldstein *et al.*, 1980; Gabius *et al.*, 2002; Zuccaro *et al.*, 2011). Even though their functions in plant–microbe interaction have not been analyzed so far, at least one lectin with WSC domains can be found among plant responsive genes in several root-associated fungi (Dore *et al.*, 2015; Kohler *et al.*, 2015). This implies a role for WSC lectins in plant colonization.

Proteins with a WSC domain were first described as cell surface sensors involved in detecting and transmitting CW status to the cell wall integrity (CWI) signaling pathway in *S. cerevisiae* (Verna *et al.*, 1997; Lodder *et al.*, 1999). These *S. cerevisiae* WSC proteins possess small C-terminal cytoplasmic domains, a single transmembrane domain, a WSC domain at the N-terminus and a periplasmic ectodomain rich in Ser/Thr residues proposed to function as mechanosensors of the extracellular matrix (Rajavel *et al.*, 1999; Philip & Levin, 2001). Proteins with WSC domain(s) and a transmembrane anchor are also involved in the activation of the CWI pathway in the yeast *Kluyveromyces lactis*, the filamentous fungi *Aspergillus nidulans*, *Neurospora crassa*, *Beauveria bassiana* and in the brown algae *Fucus serratus* (Rodicio *et al.*, 2008; Futagami *et al.*, 2011; Maddi *et al.*, 2012; Herve *et al.*, 2016; Tong *et al.*, 2016). WSC domains also are present in the fungal β1-3-exoglucanase of *Trichoderma harzianum* (Cohen-Kupiec *et al.*, 1999), suggesting that this domain mediates binding to fungal CW-associated carbohydrates. Yet, no biochemical information about their glycan interactors is available. Interestingly, also in the nematode-trapping fungus *Monacrosporium haptotylum* an expansion of genes encoding proteins with WSC domains was found. The authors proposed an involvement of these proteins in adhesion to fungal cells (Andersson *et al.*, 2013). A WSC domain also was found in human polycystin 1 (PKD1), a plasma membrane protein that is defective in autosomal dominant polycystic kidney disease (Ponting *et al.*, 1999), indicating that this domain is conserved from yeasts to mammalian cells but it is not present in higher plants.

Here we report on the biochemical proprieties, carbohydrate-binding affinities and localization of two plant responsive lectins from *S. indica*, the ~39 kDa integral CW component WSC3 with three WSC domains (*PIIN_05825*) and the previously identified 6.2 kDa plant immune suppressor *Si*FGB1 (*PIIN_03211*; Wawra *et al.*, 2016). These two lectins are induced *in planta*, bind β-glucans with diverse carbohydrate-binding motifs that share no sequence homologies to each other and have different functions during plant colonization.

Materials and Methods

Detailed description of the identification and phylogenetic analyses of lectin-like proteins in fungal genomes, fungal colonization assays, assessment of gene expression, adhesion of *Serendipita indica* spores to barley roots in the presence of WSC3, confocal microscopy, cloning of *Si*WSC3 and transformation of *S. indica*, SDS-PAGE and Western blotting, cloning and expression of *Si*WSC3-His, expression and purification of *Si*FGB1-His, FITC488 labeling of *Si*WSC3-His and native *Si*FGB1, circular dichroism spectroscopy of *Si*WSC3-His, *Si*WSC3-His pull-down assay with cell wall (CW) preparations, enzymatic extraction of CW proteins and CW stress assay in *Pichia pastoris* and primer list can be found in Supporting Information Methods S1.

Fungal strains, plant material and growth conditions

The dikaryotic *S. indica* wild-type (WT) strain DSM11827 (Leibniz Institute DSMZ-German Collection of Microorganisms and Cell Cultures, Braunschweig, Germany) and the dikaryotic *S. indica* transformants carrying a hygromycin resistance gene were cultivated at 28°C on solid or liquid complex medium (CM) with shaking at 120 rpm with or without hygromycin (80 $\mu g\ ml^{-1}$ final concentration; Carl Roth, Karlsruhe, Germany) as described in Hilbert *et al.* (2012). Additionally, a homokaryotic *S. indica* transformant carrying a geneticin resistance gene was used as reference for experiments including the *S. indica* homokaryotic transformant m5 expressing FGB1:GFP (Wawra *et al.*, 2016; GFP, green fluorescent protein). The *Colletotrichum tofieldiae* strain Ct61 (Hiruma *et al.*, 2016) was kindly provided by Paul Schulze-Lefert from the Max Planck Institute for Plant Breeding Research, Cologne and Soledad Sacristán from the Universidad Politécnica de Madrid, and propagated on solid CM supplemented with 1.5% agar in darkness at 25°C. The haploid solopathogenic *Ustilago maydis* strain SG200 was grown in liquid YEPS light (0.4% (w/v) yeast extract, 0.4% (w/v) peptone, 2% (w/v) sucrose) as described in Kamper *et al.* (2006).

For the fungal confrontation experiments *S. indica* and *Bipolaris sorokiniana* strain ND90Pr (Leibniz Institute DSMZ-German Collection of Microorganisms and Cell Cultures) were grown in liquid MYP medium (0.7% (w/v) malt extract, 0.1% (w/v) peptone, 0.05% (w/v) yeast extract) at 28°C and 120 rpm of shaking for 4 or 3 d, respectively. The mycelium of both fungi was filtered through a Miracloth filter (Merck, Darmstadt, Germany) and washed three times with sterile ddH_2O before disrupting the mycelial aggregates with a blender (Kinematica, Lucerne, Switzerland). The crushed mycelium was regenerated for 1 d at 28°C at 120 rpm of shaking in fresh MYP medium. For the confrontation assay the mycelium was again filtered through a Miracloth filter and 0.5 g each of *S. indica* and *B. sorokiniana* mycelium were mixed together, re-suspended in

5 ml sterile ddH_2O and added to 30 g of autoclaved Cologne land soil (CAS10). As a control, 1 g of filtered *S. indica* mycelium was re-suspended in 5 ml sterile ddH_2O and mixed with 30 g of soil. After 42 h at 28°C the fungal mycelium was harvested from the surface of the soil, flash frozen in liquid nitrogen and stored at −80°C until RNA was extracted.

For the fungal colonization experiments *Arabidopsis thaliana* Col-0 and *Hordeum vulgare* Golden Promise were cultivated and inoculated with fungal spores as described previously (Wawra *et al.*, 2016). Arabidopsis roots from three square petri plates each containing 20 plants were pooled per biological replicate before DNA or RNA extraction. Roots from four barley plants grown in a single jar were pooled per biological replicate.

Transmission electron microscopy and quantification of glycan labeling

The dikaryotic *S. indica* WT strain, the homokaryotic *S. indica* reference transformant, the dikaryotic *S. indica* WSC3-GFP transformant T_3 and the homokaryotic *S. indica* FGB1:GFP transformant m5 were grown on solid CM plates for 3 wk. For TEM analysis, samples were washed and subsequently fixed in 2.5% glutaraldehyde + 2% paraformaldehyde in 0.05 M sodium cacodylate buffer, pH 6.9, for 2 h at room temperature followed by an overnight incubation at 4°C. After thorough rinsing with 0.05 M sodium cacodylate buffer, the samples were post-fixed for 1 h on ice with 0.5% osmium tetroxide in 0.05 M sodium cacodylate buffer, pH 6.9, supplemented with 0.15% potassium ferricyanide. Thereafter, the samples were again thoroughly rinsed with 0.05 M sodium cacodylate buffer and dehydrated in an ethanol series from 10% to 100%, then in different ethanol : acetone mixtures and finally in 100% acetone. Subsequently, samples were infiltrated with 25% Araldite 502/EmBed 812 (EMS, Hatfield, PA, USA) in acetone. Further resin infiltration and final embedding was performed with the help of the EMS poly III, an evaporation-controlled automated embedding and polymerization device (EMS). Ultrathin sections (70–90 nm) were prepared as described previously (Micali *et al.*, 2011; Kleemann *et al.*, 2012). For the detection of β1-3-glucan, the samples were immunogold-labeled as described in Micali *et al.* (2011) using a 1 : 100 dilution of the mouse monoclonal anti-β1-3-glucan antibody (Cat. no. 400-2; Biosupplies Australia Pty, Parkville, Vic., Australia). Detection of chitin was performed using undiluted WGA conjugated with 10 nm gold particles (EY Laboratories, San Mateo, CA, USA) for 3 h at room temperature, followed by thorough rinsing with TRIS buffer and water. Sections were stained with 0.1% (w/v) potassium permanganate in 0.1N sulfuric acid for 1 min (Sawaguchi *et al.*, 2001). Transmission electron microscopy (TEM) was performed using a Hitachi H-7650 TEM (Hitachi, Krefeld, Germany) operating at 100 kV. The acquired pictures were further analyzed using the Fiji software (Schindelin *et al.*, 2012). To quantify chitin and β1-3-glucan within the fungal CW the corresponding gold particles were counted from ~ 50 TEM images per fungal strain per treatment. After counting the gold particles, the length of the CW was quantified and the number of gold particles per µm of CW was calculated for each individual image.

Quantitative assay for lectin-induced cytoagglutination

The ability of WSC3, FGB1 and WGA to aggregate fungal cells/spores was investigated for *B. sorokiniana*, *S. indica,* and *U. maydis*. *Ustilago maydis* was grown over night in 5 ml YEPS light and the OD_{600} of the culture was measured subsequently. The culture was diluted with fresh YEPS light to an OD_{600} of 0.4. *B. sorokiniana* spores were diluted to 500 spores ml^{-1} in MYP medium and *S. indica* spores were diluted to 50 000 spores ml^{-1} in CM. One hundred microliters of the cell/spore solutions were transferred to individual wells of a 96-well plate. The recombinant *Si*WSC3-His was sterile-filtrated using a 0.22-µm filter and was added to the individual wells with a final concentration of 10 µM. As controls, 10 µM WGA-AF594 (Invitrogen), 10 µM native FGB1 or 10 µM WSC3-FITC488 were added to the individual wells. As a mock control, sterile ddH_2O was used. Sterile ddH_2O was added to a final volume of 150 µl to each well.

Phenotypic assessment of *U. maydis* sporidias was done microscopically after 4 h of incubation at 28°C with 250 rpm of shaking. The agglutination effect was quantified by counting the aggregated *U. maydis* cells relative to the total number of cells. An aggregate was defined as a structure with two or more cells being in direct contact with each other but not connected, as for example in dividing cells.

Fluorescence labeling of WSC3-His and nFGB1 and Microscale Thermophoresis (MST)

Fluorescent labeling of WSC3 for MST measurements was done using the Biotinum CF594 succinimidyl ester protein labeling kit (#92216) according to the manufacturer's protocol. Native FGB1 was labeled using the Lightning-Link® (R-PE) Kit (703-0015; Innova Biosciences, Expedeon, San Diego, CA, USA) according to the supplier's instructions. Data were recorded on a Monolith NT.115 instrument in standard coated capillaries using a fluorescence excitation of 510–550 nm and emission detection at 560–590 nm. WSC3-His CF594 was used at a concentration of 60 nm (for pre-tests) or 500 nM (for binding affinity measurements) with the MST power set to high at a laser intensity of 60%. Buffers were either 37.5 mM MES + 75 mM NaCl + 0.05% Tween 20 pH 5.0 or phosphate buffered saline containing 0.05% Tween 20 at pH 7.4. For nFGB1 R-PE a protein concentration of 20 nM was used in 25 mM MES buffer pH 5.0 containing 1.25 mg ml^{-1} BSA, 0.25% glycerol, 0.5% Tween 20 and 50 mM NaCl. Binding affinities were measured through a series of 16 successive 2× dilutions of the ligand stock solutions dissolved in the respective assay buffers.

Isothermal titration calorimetry (ITC)

Isothermal titration experiments were performed using a VP-ITC instrument at 20°C. The instrument was heat-pulse-calibrated and the protein samples were extensively dialyzed against water

before use. Titrant stock solutions were prepared with the same batch of water as used for dialysis. All solutions used were degassed before filling the sample cell and syringe. The ITC stirring speed was set to 300 rpm; the feedback gain mode was set to medium. Because the initial injection generally delivers inaccurate data, the first step was omitted from the analysis. The collected data were analyzed using the program ORIGIN (MicroCal, Malvern Panalytical, Malvern, UK) and binding isotherms were fitted using the binding model provided by the supplier. Errors correspond to the SD of the nonlinear least-squares fit of the data points of the titration curve. For the titration of WSC3-His to laminarin a 18.5 μM protein bait solution was titrated with a 1 mM laminarin solution. The first injection (1 μl) was followed by 29 titrations with 6 μl each and 150 s of spacing. The titration curve was baseline-corrected and subtracted with the data from the control titration of the laminarin stock into water. For testing of chitohexaose binding a WSC3-His bait concentration of 16 μM was used with a chitohexaose stock solution of 1.5 mM. Laminarihexaose and gentiobiose (1 mM stock each) were titrated against 20 μM WSC3-His bait solution.

Enzymatic preparation of debranched beta-glucan from laminarin

In order to generate linear β1-3-glucan without β1-6-glucose side chains we used a biocatalytic strategy as described previously (Becker *et al.*, 2017). In brief, 100 mg of laminarin from *Laminaria digitata* (Sigma) was hydrolyzed overnight at 37°C with 100 nM purified enzyme (~5 μg ml^{-1}) of a β1-6-exo glucosidase of glycoside hydrolase family 30 (GH30) that specifically removes the β1-6-linked glucose side chains from laminarin. This reaction leads to glucose and the linear β1-3-glucan. Completeness of the conversion was confirmed by testing the activity of a β1-3-endo glucanase of family GH17 that only cleaves undecorated, linear β1-3-glucan (Becker *et al.*, 2017; Unfried *et al.*, 2018) and shows little activity on the native yet high activity on the debranched laminarin. The reaction was stopped by boiling the sample for 5 min at 100°C. Precipitated protein was removed by filtration through 0.2 μm Costar Spin-X Filters (Corning, Kaiserslautern, Germany). The glucose was separated from the β1-3-glucan by size exclusion chromatography using a HiTrap Desalting column (GE Healthcare, Solingen, Germany) according to the manufacturer's instructions. The column was equilibrated and eluted with Milli-Q water. The solution was dried in vacuum overnight at 45°C to obtain a white powder. The enzymatic digestion with both enzymes and absence of glucose in the final product was recorded by high performance anionic exchange chromatography with pulsed amperometric detection (HPAEC-PAD) on a Dionex system (Unfried *et al.*, 2018).

Results

SiWSC3 and SiFGB1 alter CW properties

Comparative genomics and phylogenetic analysis identified a strong taxa-specific expansion for the lectin-like WSC proteins in some fungal genomes, symptomatic of a rapid evolution (Figs 1, S1, S2; Table S1). This was especially evident in the sebacinoid fungi and in the saprotrophic white rot fungus *Auricularia subglabra* (Figs 1, S1, S2). From transcriptional analyses we identified a plant-responsive clade of WSC lectin-like members in the sebacinoid fungi (Lahrmann *et al.*, 2015) (Fig. 1b,c, S1). Among this subset *SiWSC3* (*PIIN_05825*) was highly transcriptionally induced and was selected for further functional characterization. Expression analysis by quantitative reverse transcription polymerase chain reaction (qRT-PCR) confirmed the expression pattern of *SiWSC3* during plant root colonization in Arabidopsis and barley with stronger expression in the latter. Additionally, induction of *SiWSC3* was detected during contact of *S. indica* with the plant pathogenic fungus *B. sorokiniana* in a soil confrontation assay (Fig. 2a). Because WSC proteins were proposed to bind to the CW of fungi and *Si*WSC3 harbors a predicted secretion signal peptide, we hypothesized that *Si*WSC3 may localize to the CW of *S. indica.* To study its subcellular localization the *SiWSC3* gene was expressed as fusion with a C-terminal GFP tag under the control of the *S. indica* FGB1 promoter which is highly active *in planta* and in complex medium (CM) but less active in other axenic media (Wawra *et al.*, 2016). Mycelium and culture filtrate of five independent *S. indica* transformants grown in CM and MYP were tested for secretion of the *Si*WSC3:GFP fusion protein (Fig. 2b). The highest amount of full-length *Si*WSC3:GFP fusion protein was detected in the mycelial sample of the transformants T_1 and T_3 grown in CM. The full-length fusion protein was not detectable by Western blot in the culture filtrates but the presence of free GFP indicated that secretion occurred. The full-length and cleaved *Si*WSC3 protein versions most likely remained bound to carbohydrates present at the surface of the fungal cells in the mycelium fraction (Fig. 2b). To verify this hypothesis cytological analysis were performed with the *S. indica* transformant T_3 which produced a higher amount of the *Si*WSC3:GFP fusion protein and the transformant T_2 for which no band was detected in the Western blot. Additionally, the fungal transformant m5, harboring a *Si*FGB1:GFP fusion construct under the control of the *S. indica* FGB1 promoter, was used as control. *Si*FGB1:GFP was previously shown to localize to the fungal CW and to additionally be one of the most abundant proteins secreted by *S. indica* in the culture filtrate (Wawra *et al.*, 2016). The *Si*WSC3:GFP fluorescence signal co-localized with the signal of the chitin-binding lectin WGA-AF594 at the CW for transformant T_3 (Fig. 2c), whereas no specific fluorescence could be detected for the transformant T_2 using identical confocal laser scanning microscope settings (Fig. 2d). *Si*FGB1:GFP fusion showed in addition to the CW localization, a strong signal at the fungal septa and in structures that resembled the endoplasmic reticulum (Fig. 2e) (Rico-Ramirez *et al.*, 2018). The localization of the *Si*WSC3:GFP and *Si*FGB1:GFP fluorescence signal at the fungal CW suggests that modification of both lectins at the C-terminus does not severely impact ligand–protein binding.

The effects of overexpression of these lectins on the CW polysaccharide composition was assessed by transmission electron microscopy (TEM) using chitin- and β1-3-glucan-specific immunogold-labeling (Mayhew, 2011). Quantitative analyses were performed for the mycelia of *S. indica* FGB1:GFP transformant m5 and the WSC3:GFP transformant T_3 and

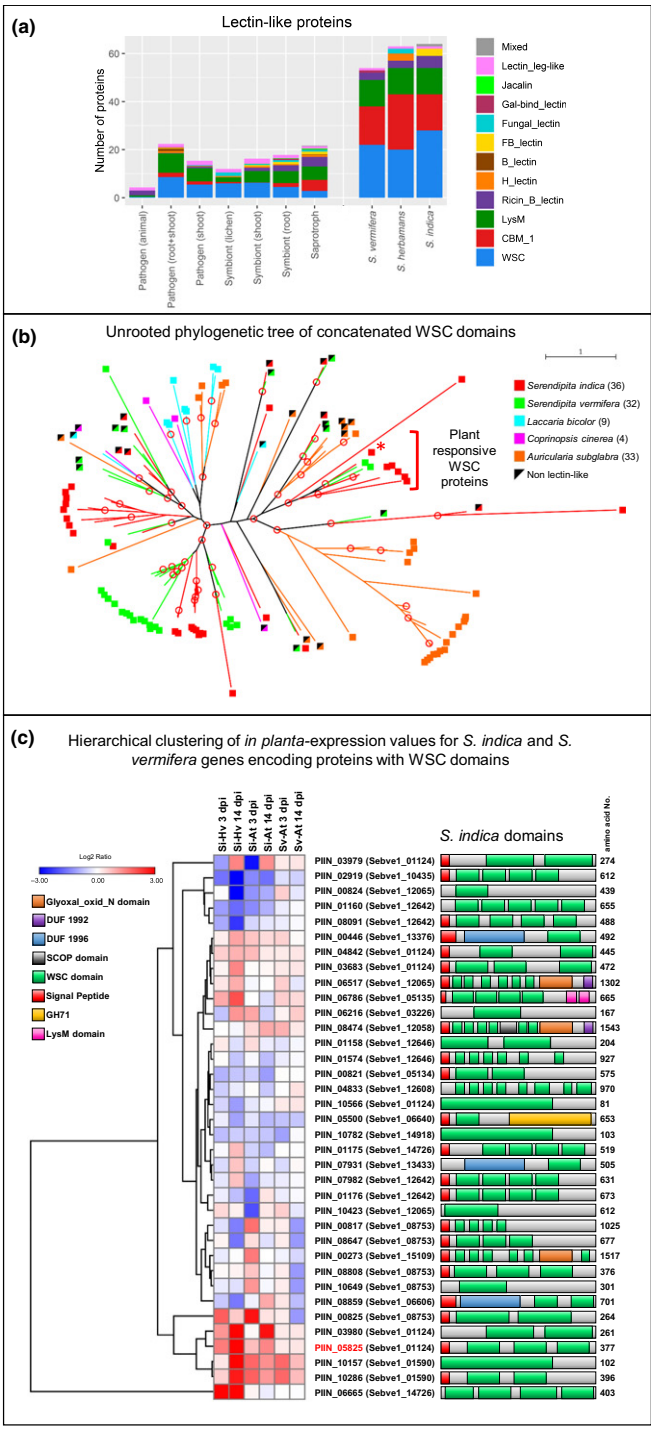

Fig. 1 Expansion of genes encoding for proteins with WSC domains in sebacinoid fungi and their expression during plant colonization. (a) Number of predicted lectin-like proteins in the genome of sebacinoid fungi compared to the average values of these proteins in different fungal genomes that are grouped based on their predominant lifestyle and colonized tissue into symbionts (root, shoot, lichens), plant pathogens (shoot, root + shoot), animal pathogens, saprotrophs, and *Serendipita indica*, *S. vermifera* and *S. herbamans*. Functional protein domains involved in carbohydrate binding were predicted from 79 fungal genomes (listed in Supporting Information Table S1) using the Pfam database (Finn *et al.*, 2010). Lectin-like proteins were defined as proteins that only contain one or a combination of the shown nonenzymatic domains and were identified from PfamScan output with custom Java applications. The number of proteins shown is the average over all fungal genomes belonging to one of the groups (*S. indica*, *S. vermifera* and *S. herbamans* were not included in the average). Bar charts were created using GNUPLOT (http://www.gnuplot.info). Lectins with CBM1 domains are absent in the genomes of animal pathogens and over-represented in plant saprotrophs and sebacinoid fungi. Lectins with WSC domains are over-represented in the sebacinoid fungi. (b) Phylogenetic relationships among proteins with WSC domains calculated using concatenated WSC domains in PHYML (Guindon *et al.*, 2010). Black triangles indicate proteins with at least one additional functional domain different from the WSC domain. Red asterisk indicates PIIN_05825. Approximate likelihood ratios were omitted for reasons of better readability and are shown in Fig. S2. Clades entirely composed of monospecific representatives suggest a rapid expansion for some of the proteins, such as the plant-responsive one where the PIIN_05825 is situated. Nodes supported by bootstrap values > 80% are marked with red-outlined circles calculated using the approximate likelihood ratio test (aLRT) for branches with a cut-off of 90. (c) Domain architecture and expression profile of *S. indica* proteins with WSC domains. Respective Pfam domains are color-coded: red, signal peptide; green, WSC domain; orange, Glyoxal_oxid_N domain; blue, DUF1996 domain; yellow, GH71 domain; purple, DUF1929 domain; pink, LysM domain; black, SCOP domain. The heat map shows the $\log_2$-fold changes for the expression of *S. indica* and *S. vermifera* genes encoding for proteins with WSC domains during colonization of *Arabidopsis thaliana* (*At*) roots at 3 d post inoculation (dpi) and 14 dpi and of *Hordeum vulgare* (Hv) roots at 3 dpi and 14 dpi. Fold-change levels were obtained through normalization of the data to *Serendipita* spp. grown on 1/10 PNM. Transcriptome data for *S. indica* and *S. vermifera* resulted from microarray experiments with three biological replicates for each time point published in Lahrmann *et al.* (2015) and are deposited at GEO (*S. indica*: GSE60736; *S. vermifera*: GSE60736).

corresponding controls labeled either with gold-conjugated WGA or with the β1-3-glucan-specific antibody. Whereas gold-conjugated WGA labels for chitin was constant in all fungal samples (Figs 2f, S3), the amount of gold labels for β1-3-glucan was significantly increased in the *Si*FGB1:GFP overexpressing transformant m5 compared to the control (Figs 2g, S3). The data obtained for the transformant m5 corroborate previous results obtained by NMR where the ratio between chitin and glucan was found to be altered in the CW of this fungal transformant (Wawra *et al.*, 2016). The amount of gold labels for β1-3-glucan was significantly reduced in the CWs of the *Si*WSC3:GFP overexpressing transformant T_3 which could result from alteration in glucan composition or in availability of β1-3-glucan to the antibodies. In both cases deregulation of *SiWSC3* leads to alteration of CW properties which are different from those observed for *Si*FGB1. As anticipated by the confocal microscopy analysis, TEM analyses indicate that chitin is found prevalently at the CW of *S. indica* hyphae (Figs 2f, S3), whereas β1-3-glucan also is abundantly present/exposed at the septa and in the septal pore swellings of the dolipore (Figs 2g, S3).

SiWSC3 and SiFGB1 bind to β-glucan polysaccharides in a different manner

In order to biochemically characterize the *Si*WSC3 protein, a His-tag fusion (*Si*WSC3-His) was heterologously produced in the yeast *Pichia pastoris* under the control of the *AOX1*

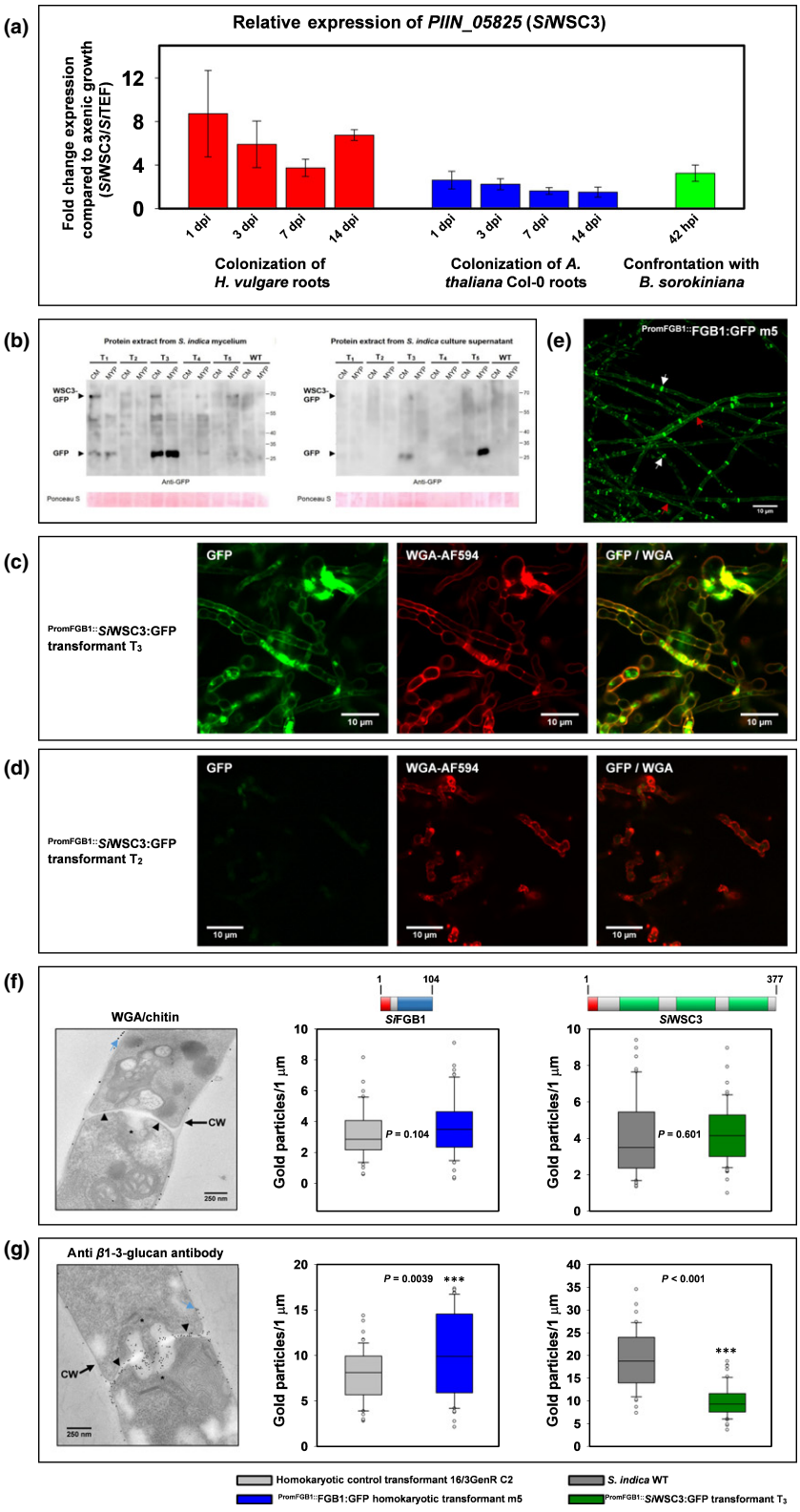

promoter. Western blot analysis and enzymatic deglycosylation revealed that this protein is abundantly secreted and is glycosylated in this fungus with an apparent retention on SDS-PAGE corresponding to a molecular weight of ~55 kDa before and ~39 kDa after deglycosylation (Fig. S4a,b). Additionally, in *P. pastoris* expression of *Si*WSC3-His leads to its incorporation into the CW and to increased resistance to the CW stressors Calcofluor White and Congo Red (Fig. S4c,d).

Fig. 2 *SiWSC3* is transcriptionally induced during root colonization and during contact with a root pathogen and localizes to the *Serendipita indica* cell wall. (a) Expression of *SiWSC3* quantified by quantitative reverse transcription polymerase chain reaction (qRT-PCR) during root colonization of *Hordeum vulgare* (red bars) and *Arabidopsis thaliana* (blue bars) or during contact with the root pathogenic fungus *Bipolaris sorokiniana* (green bar) in soil at the indicated times. The expression of *SiWSC3* was calculated using the $2^{-\Delta\Delta Ct}$ method relative to the expression of *Si*TEF. Fold changes in *SiWSC3* expression during colonization of *H. vulgare* and *A. thaliana* and in confrontation with *B. sorokiniana* were calculated using the *SiWSC3* expression levels after 5 d growth on 1/10 PNM medium, 7 d growth on ½ MS or 2 d growth in soil, respectively. Error bars indicate ± SE of the mean calculated from four biological replicates. dpi, d post-inoculation; hpi, h post-inoculation. (b) Western blot detection of *Si*WSC3-GFP with an anti-GFP antibody in mycelia (left) and culture filtrates (right blot) of five *S. indica* transformants and wild-type (WT) strain grown in complex medium (CM) or MYP medium. The band at *c*. 70 kDa corresponds to the *Si*WSC3:GFP fusion protein (highlighted in the blot; GFP, green fluorescent protein) and the band at *c*. 30 kDa corresponds to free GFP after cleavage of the fusion protein. (c) Subcellular localization of *Si*WSC3:GFP produced in *S. indica* transformant T_3 under the control of the *Si*FGB1 promoter grown in CM using confocal microscopy. A specific fluorescence signal (green) is visible at the septa and cell walls. Red shows the chitin stain WGA-AF594. (d) Confocal microscopy of the negative control transformant T_2 originating from the same transformation event as the transformant T_3. (e) Subcellular localization of *Si*FGB1:GFP produced in *S. indica* transformant m5 under the control of the FGB1 promoter grown in CM using confocal microscopy. A strong specific fluorescence signal (green) is visible at the septal rings (white arrowheads) and in the endoplasmic reticulum (red arrowheads). Bars, 10 μm. (f, g) Relative quantification of chitin (f) and β-glucan (g) in the cell wall of *S. indica* by immunogold-transmission electron microscopy (TEM) and representative TEM images. Chitin was visualized by gold conjugated wheat germ agglutinin (WGA) and β1-3-glucan was visualized by a primary monoclonal mouse antibody with the help of a gold conjugated secondary anti-mouse antibody. Number of gold particles at the cell wall were counted from at least 48 TEM images for each fungal strain. Immuno-gold particles in the septa and dolipore were omitted from the analysis. CW, cell wall; asterisk, dolipore; black arrowheads, septa; blue arrowheads, show exemplarily gold particles; light grey bar, homokaryotic reference transformant; blue bar, homokaryotic *Si*FGB1:GFP transformant m5; dark gray bar, dikaryotic WT reference strain; green bar, dikaryotic *Si*WSC3:GFP transformant T_3. Significances were calculated by Student's *t*-test: ***, $P < 0.005$. Bars, 250 nm (see Supporting Information Fig. S3 for more details). Schematic representations of FGB1 and WSC3: red, predicted signal peptide; blue, FGB1 carbohydrate-binding domain as predicted from alignment analysis (Wawra *et al.*, 2016); green, WSC domain as predicted by SMART (http://smart.embl-heidelberg.de). Box–whisker plots: horizontal lines, median; circles, outliers; whiskers, minimum and maximum of 1st and 4th quartile.

In order to determine whether *Si*WSC3 specifically binds to fungal CW polysaccharides a pull-down experiment was performed using insoluble, protein-free polysaccharide preparations of *H. vulgare* and *S. indica* CWs. In this experiment, *Si*WSC3-His co-precipitated with the *S. indica* but not with the *H. vulgare* CW polysaccharide preparations (Fig. S4e). This suggests a specificity of *Si*WSC3 for an oligosaccharide or polysaccharide of fungal origin as it was shown previously for *Si*FGB1 (Wawra *et al.*, 2016). Therefore, the heterologously produced *Si*WSC3-His was used for ITC analysis to determine its affinity to different oligo- and polysaccharide ligands possibly found in fungal CWs. Accordingly, a soluble β1-3-glucan with β1-6-linkages consisting of ~30 glucose units (laminarin), a linear β1-3-glucan hexamer (laminarihexaose), a β1-6-linked glucose dimer (gentiobiose) and a chitin octamer (chitooctaose) were included in the survey. Upon titration of the soluble laminarin to *Si*WSC3-His in water an exothermal binding reaction was observed with a K_d value of 12.5 μM ± 8.8 μM. No significant binding was detected for the other polysaccharides tested (Fig. 3a). Circular dichroism (CD) spectroscopy showed that neither laminarin binding nor pH affected the secondary structure of *Si*WSC3 (Fig. S5), suggesting that *Si*WSC3 has a preformed carbohydrate-binding site that can accommodate the β-glucan ligand. The ITC measurement also revealed an apparent stoichiometry for the reaction of 1 : 3 meaning that one *Si*WSC3 binds three β1-3/1-6-glucan molecules. This suggests that each of the three WSC-domains may bind one β1-3/1-6-glucan molecule. Alternatively, it is possible that the three WSC domains act together to increase the binding affinity to higher order β-glucan structures such as the triple-helical structure found for laminarin in solution (Sletmoen & Stokke, 2008; Kanagawa *et al.*, 2011). Because *Si*WSC3 did not bind to any of the shorter glucose oligomers, which cannot assume a triple-helical conformation in solution, it is unclear whether the fungal specific β1-6-glycosidic bonds are important for the binding of *Si*WSC3-His to laminarin. To clarify if the β1-6-side chains of laminarin are required for binding to WSC3 and FGB1, we performed carbohydrate-binding studies in aqueous solution with microscale thermophoresis (MST). We tested laminarin and size exclusion chromatography purified debranched laminarin after treatment with the *Fb*GH30 enzyme derived from the bacterium *Formosa* sp. strain B. This enzyme was previously shown to specifically hydrolyze the β1-6-linked glucose side chains of laminarin (K_M: 3.1 ± 0.2 mM and K_{cat}/K_M: 21124 $M^{-1}s^{-1}$) producing linear β1-3-glucan (Becker *et al.*, 2017; Unfried *et al.*, 2018). The MST analysis at pH 5 showed that whereas FGB1 binds to native laminarin this lectin does not bind to debranched laminarin. WSC3 on the contrary can bind to native and debranched laminarin with similar affinities (Figs 3b, S5, S6). These data suggest that FGB1 but not WSC3 requires the β1-6 side chains of laminarin for efficient binding. This is in agreement with the fact that FGB1 but not WSC3 can bind to gentiobiose, a disaccharide composed of two units of D-glucose joined with a β1-6 linkage (Fig. 3a and Wawra *et al.*, 2016).

A number of additional potential ligands for WSC3 were explored using MST analyses at two different pH levels with the following carbohydrates: linear β1-4 linked (Glc)4 backbone carrying 3 glucose (Glc) units attached to this backbone by β1-6 glycosidic bonds (Xyloglucan heptasaccharide, Megazyme O-X3G4); the linear β1-4 linked Glc pentamer (Cellopentaose, Megazyme O-CPE); Glcβ1-3Glcβ1-4Glcβ1-3Glc tetramer (Cellotriosyl-glucose, Megazyme O-BGTETB); a mixture of Glcβ1-4Glcβ1-3Glcβ1-4Glc and Glcβ1-3Glcβ1-4Glcβ1-4Glc tetramers (Megazyme O-BGTETC, Cellobiosyl-cellobiose + Glucosyl-cellotriose;); as well as Galα1-4Galβ1-4Glc trimer (Globotriose, IsoSep AB, 35/03). In this screening WSC3 did not bind to any of the above-mentioned sugars with a micromolar affinity apart from the control laminarin at pH 5.5 but not at pH 7.4 (Figs S5, S6).

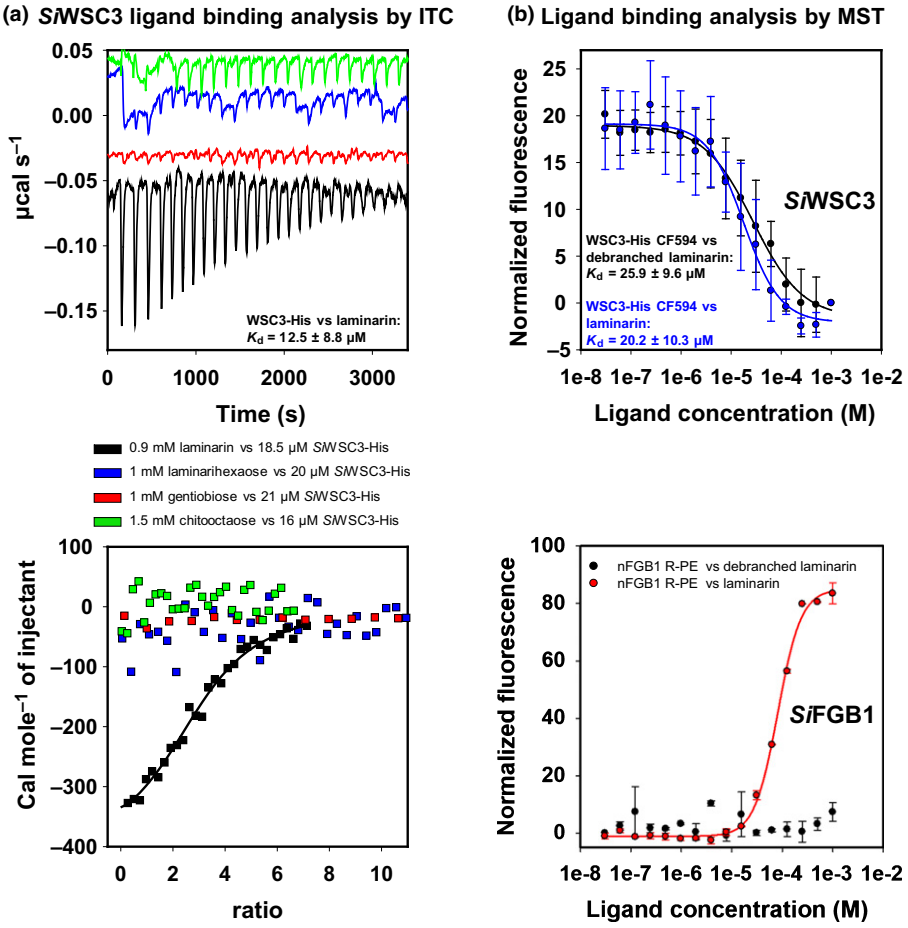

Fig. 3 *Si*WSC3 binds to linear long-chain β1-3-glucan, whereas *Si*FGB1 requires β1-6-glucose linkages for efficient binding. (a) Isothermal titration calorimetry (ITC) of chitooctaose (green), laminarihexaose (blue), gentiobiose (red) and laminarin (black) in the presence of *Si*WSC3-His. The data for the binding of *Si*WSC3-His to laminarin were fitted by a single-binding-site-model (black line lower plot) and used to calculate the following parameters for the reaction using a molecular mass for laminarin of *c*. 4800 Da (Smith *et al.*, 2018): $N = 3.1 \pm 0.0967$; $K = 8 \times 10^4 \pm 1.13 \times 10^5\ M^{-1}$, ($K_d = 12.5\ \mu M \pm 8.8\ \mu M$), $\Delta H = -407.3 \pm 18.25$ cal mol^{-1} and $\Delta S = 21.1$ cal mol^{-1} deg^{-1}. All solutions were prepared in water, data were baseline corrected and results of the corresponding control titrations of the ligand into water were subtracted. (b) *Si*WSC3 and *Si*FGB1 binding analysis to laminarin and debranched laminarin by MST (see Supporting Information Figs S5, S6 for more details). Error bars ± SD from three technical replicates.

Taken together the affinity measurements with ITC and MST lead to the conclusion that the natural substrate for *Si*WSC3 might be a long-chain β1-3-glucan with a higher order structure. This also suggests that in CW preparations of barley roots long-chain β1-3-glucans are not present or not accessible to *Si*WSC3. Indeed synthesis of β1-3-glucans have been reported in barley only during the transient production of callose (Chowdhury *et al.*, 2014).

The multivalent SiWSC3 but not SiFGB1 agglutinates fungal cells

Hyphae interact with soil particles, roots and soil microbes forming a filamentous network that promotes foraging for soil nutrients. Thus, adhesion is an important hyphal feature during interaction with roots and other fungi. To test if the addition of *Si*WSC3-His or *Si*FGB1would have an effect on fungal cell adhesion we incubated these two lectins with the filamentous basidiomycete *S. indica*, the yeast basidiomycete *U. maydis* or the filamentous ascomycete *B. sorokiniana*, spanning a considerable degree of CW diversity in their compositions and molecular architectures. The chitin-binding antifungal lectin WGA served as control protein (Mirelman *et al.*, 1975; Wawra *et al.*, 2016). The growth phenotypes of the fungi were assessed microscopically after overnight growth for *S. indica* and *B. sorokiniana* and after 4 h of growth for *U. maydis*. *Si*WSC3-His displayed a strong agglutination effect on all tested fungi whereas *Si*FGB1 did not. WGA also led to the formation of fungal cell aggregates but less dense compared to those produced in the presence of *Si*WSC3-His (Fig. 4a). Because the filamentous growth of *S. indica* and *B. sorokiniana* complicates the quantification of the lectin-induced agglutination of *Si*WSC3, a statistical analysis was performed by calculating the percentage of *U. maydis* sporidia included in aggregates relative to the total number of sporidia (Fig. 4b). Whereas *Si*FGB1 did not significantly increased agglutination compared to the mock treatment, *Si*WSC3-His and WGA increased agglutination of fungal cells remarkably. The ability of *Si*WSC3 to agglutinate cells is likely due to its multivalent nature compared to *Si*FGB1 with just one functional carbohydrate-binding domain. These results argue in favor of long-chain β1-3-glucans being present in the CWs of these fungi.

In order to assess if these lectins mediate fungal adhesion to roots, *S. indica* chlamydospores were incubated with barley roots in a solution containing either native *Si*FGB1 or *Si*WSC3-His dissolved in water or in buffer. Addition of the lectins had no effect on spore adhesion to the roots (Fig. 4c) and the incubation with *Si*WSC3-His did not negatively affect *S. indica* growth (Fig. S7a). To explore the effect of *Si*WSC3 on colonization, barley roots were inoculated with *S. indica* spores in both the presence and absence of 10 µM *Si*WSC3-His and grown for 3 d

under sterile conditions. As positive control barley roots were inoculated with *S. indica* spores in presence and absence of 10 μM disulfide bonded *Si*FGB1-His heterologously produced in *E. coli*. Subsequently, gDNA was extracted and the colonization rate was measured by quantification of the relative amount of fungal DNA to plant DNA by qRT-PCR. This pharmacological experiment resulted in a significant increase in fungal colonization in the presence of *Si*FGB1-His as shown previously for the native *Si*FGB1 (Wawra *et al.*, 2016), whereas *Si*WSC3-His showed no effect on the *S. indica* colonization rate (Fig. 4d). Similarly, the use of the *S. indica* WSC3 overexpression transformants did not result in enhanced colonization (Fig. S7b). This suggest that WSC3 is not capable of suppressing plant immunity as observed for FGB1 and it is possibly involved in fungal CW reinforcement and cohesive adhesion between hyphal cells.

β-glucan-binding lectins as a nondestructive molecular probe for fungi in complex samples

The most abundant building block of fungal CWs is glucan, which often makes up to 50–60% DW (Fesel & Zuccaro, 2016a). Although β1-3-glucose chains also can be found in the CW of plants in the form of callose, polymers containing β1-6-glycosidic bonds have only been found in the CW of fungi and members of the phylum Stramenopiles, such as in some genera of oomycetes. It is proposed that the β1-6-glycosidic bonds are responsible for connecting glucan chains with each other and thus for conferring rigidity to the CW (Bowman & Free, 2006; Latge, 2007). The multi-branched β-glucans can be firmly bound to the CW or loosely bound and accumulate around the fungus as gelatinous material. The characterization of these two novel high affinity glucan binding lectins prompted us to test their ability to specifically detect fungal-derived glycans in complex samples. FITC488 conjugates of native *Si*FGB1 and *Si*WSC3-His were generated and used as probes to detect the fungal CW in different root-associated fungi such as the endophytes *S. indica* and *C. tofieldiae* and the plant pathogen *B. sorokiniana* during root colonization. Cytological analysis showed that *Si*WSC3-FITC488 did not localize to the fungal or plant CWs. Subsequent, agglutination experiments with the conjugated *Si*WSC3 protein showed that the labeling (with a labeling efficiency calculated at ~55%) had a significant effect on the ability of this protein to agglutinate fungal cells and thus likely on the interaction of *Si*WSC3 to β-glucan (Fig. 4b), explaining the absence of binding at the fungal CW in confocal microscopy. A reason could be that the covalent carboxamide bonds formed with primary amines of the protein during the reaction with 5-FAM-X [6-(Fluorescein-5-carboxamido) hexanoic acid, succinimidyl ester] belonged either to an amine group important for the interaction with the ligand and/or to a structurally important amino acid side chain (Holmes & Lantz, 2001). WSC3 labeling with CF594, as used in MST analyses, did not severely impair binding to laminarin but produced artefacts during confocal imaging in complex biological samples and was not further used in cytological analyses. By contrast, *Si*FGB1-FITC488 bound efficiently to the CWs of all three fungi (Fig. 5). Chitin was hardly stainable with WGA-AF594 in *B. sorokiniana* and *C. tofieldiae*, suggesting that these two fungi do not expose chitin *in planta*. Yet their CWs were stainable with *Si*FGB1-FITC488, indicating that β-glucans are a good target for molecular probes. The remarkably small size of *Si*FGB1 makes it more permeable compared to glucan antibodies or larger lectins such as WGA, staining more efficiently the hyphae inside living colonized host cells during fluorescence live cell imaging. In our study, the use of *Si*FGB1-FITC488 revealed the presence of a thick and diffuse polysaccharide matrix around the hyphae of these fungi. The matrices were visible around the hyphae outside of the host cells but also were observed frequently around intracellular hyphae (Figs 5, S8a–c). During host cell penetration the fungal matrix diffuses around the penetration zone (clearly visible in Fig. S8a), suggesting that it is not tightly bound. After washing of the hyphae with water the matrix was no longer visible, showing that it is water soluble and loosely attached to the fungal surface (Fig. S8d). Due to its water solubility we could not detect this matrix regularly around fungal hyphae of *S. indica* with β-glucan antibody in the TEM analysis. Nevertheless, in some of the TEM sections the matrix was still visible and stained by the antibody, indicating that this matrix is made of β1-3/1-6-glucans (Fig. S9). These data show that the secretion of a fungal β-glucan matrix is a common feature of root-associated fungi independent of their lifestyle and taxonomy.

Discussion

Biochemical properties of FGB1 and WSC3

The number of biochemically characterized β-glucan binding lectins from fungi is very limited (Wawra *et al.*, 2016). WSC domains are conserved from yeasts to mammalian cells but their sugar ligand/s are unknown. The aim of this study was to characterize the binding ability of a plant responsive WSC domain containing lectin from *Serendipita indica* and to compare its properties with those of the recently described β-glucan binding lectin *Si*FGB1 which possesses a structurally unrelated carbohydrate-binding domain. The performed isothermal titration calorimetry (ITC), circular dichroism (CD) spectroscopy and microscale thermophoresis (MST) measurements represent the first experimental proof that long chain β1-3-glucans are the preferred polysaccharide bound by proteins with WSC domain(s). *Si*WSC3 binds β-glucan with a K_d value of 12.5 μM ± 8.8 μM and a molar ratio of protein to substrate of 1 : 3. Although the affinity of WSC3 to β-glucan is lower compared to the K_d value of ~100 nM for the native *Si*FGB1 (Wawra *et al.*, 2016) this is still a strong binding affinity as many lectins bind in the millimolar range (Navarra *et al.*, 2017). Our data show that the higher affinity of *Si*WSC3 for longer carbohydrate polymers most likely requires a complex 3D polysaccharide structure. This is in contrast to *Si*FGB1 which requires the presence of β1-6 side chains and can also bind to the glucose dimer gentiobiose (Wawra *et al.*, 2016). In common with other lectins, *Si*WSC3 seems to have a preformed carbohydrate-binding site, which can accommodate the β-glucan ligand without undergoing a strong conformational change in its structure. This feature seems to minimize the energetic penalty paid upon binding to carbohydrate ligands

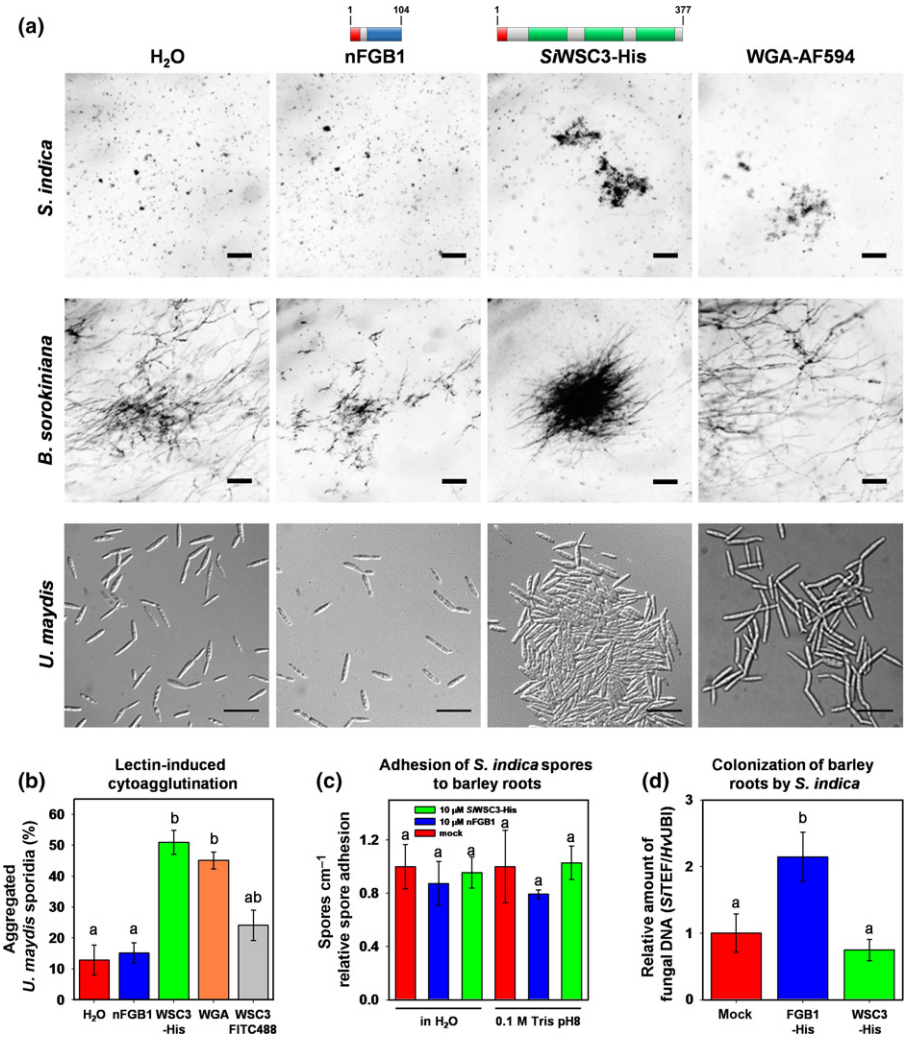

Fig. 4 Addition of *Si*WSC3 induces the formation of multicellular aggregates in different fungi but does not lead to hypercolonization of plant roots. (a) Lectin-induced cytoagglutination of *Serendipita indica*, *Bipolaris sorokiniana* and *Ustilago maydis* grown in the presence of 10 μM native *Si*FGB1 (nFGB1), 10 μM *Si*WSC3-His, 10 μM WGA-AF594 or water in complex medium. Pictures of *S. indica* and *B. sorokiniana* were taken after 16 h of growth using a Leica M165 FC stereo microscope. *Ustilago maydis* was grown for 4 h before pictures were taken using a Leica DM2500 light microscope. Bars: (*S. indica* and *B. sorokiniana*) 500 μm; (*U. maydis*) 25 μm. Schematic representations of FGB1 and WSC3: red, predicted signal peptide; blue, FGB1 carbohydrate-binding domain; green, WSC domain. (b) Lectin-induced cytoagglutination of *U. maydis* sporidia. The degree of *U. maydis* aggregation was quantified by calculating the percentage of aggregated cells relative to the total number of cells. Red bar, water; blue bar, 10 μM native *Si*FGB1; green bar, 10 μM *Si*WSC3-His; orange bar, 10 μM WGA-AF594; grey bar, 10 μM *Si*WSC3-His-FITC488. Error bars show ± SD of four biological replicates. Native *Si*FGB1 had no effect on fungal cell aggregation, whereas WSC3-His and WGA-AF594 treatment significantly increased the number of aggregated cells. Letters indicate independent groups according to an unpaired Student's *t*-test ($P < 0.05$; $n > 100$). (c) Adhesion of *S. indica* spores to barley roots were calculated by counting the number of attached spores to the root surface from images acquired by confocal laser scanning microscopy. *Serendipita indica* spore solution was mixed either with an equal volume of water or Tris buffer pH 8 (mock, red bars), 10 μM nFGB1 (blue bars) or 10 μM *Si*WSC3-His (green bars) diluted in water or in Tris buffer pH 8. Error bars represent ± SE of the mean of three biological replicates. No significant differences between the treatments were observed using an unpaired Student's *t*-test ($P < 0.05$, indicated by the letter 'a'). (d) Fungal colonization of barley roots. *Serendipita indica* spore solution was mixed either with water (mock, red bar), 10 μM recombinant His tagged FGB1 diluted in water (blue bar) or 10 μM *Si*WSC3-His diluted in water (green bar) and the colonization rate was quantified by quantitative reverse transcription polymerase chain reaction (qRT-PCR) measuring the relative amount of fungal gDNA (*SiTEF*) compared to plant gDNA (*HvUBI*) at 3 d post-inoculation (dpi). The colonization rate was normalized to the respective mock-treatment which was set to 1. Error bars represent ± SE of the mean of at least six biological replicates. No significant difference between the mock and *Si*WSC3-His treatment was observed whereas recombinant FGB1-His significantly increased colonization. Letters indicate independent groups according to an unpaired Student's *t*-test ($P < 0.05$).

(Kanagawa *et al.*, 2011). Remarkably, binding of the ligand to *Si*FGB1 leads to dramatic secondary structural changes which are thought to be necessary for the immunosuppressive function of this protein *in planta* (Wawra *et al.*, 2016). Mutational analyses of FGB1 will help proving this hypothesis in future studies.

FGB1 and WSC3 functions

Several lectins from phytopathogenic fungi have been characterized including beta-trefoil lectins from *R. solani* and *S. sclerotiorum*, actinoporin-like lectins from *S. rolfsii* and

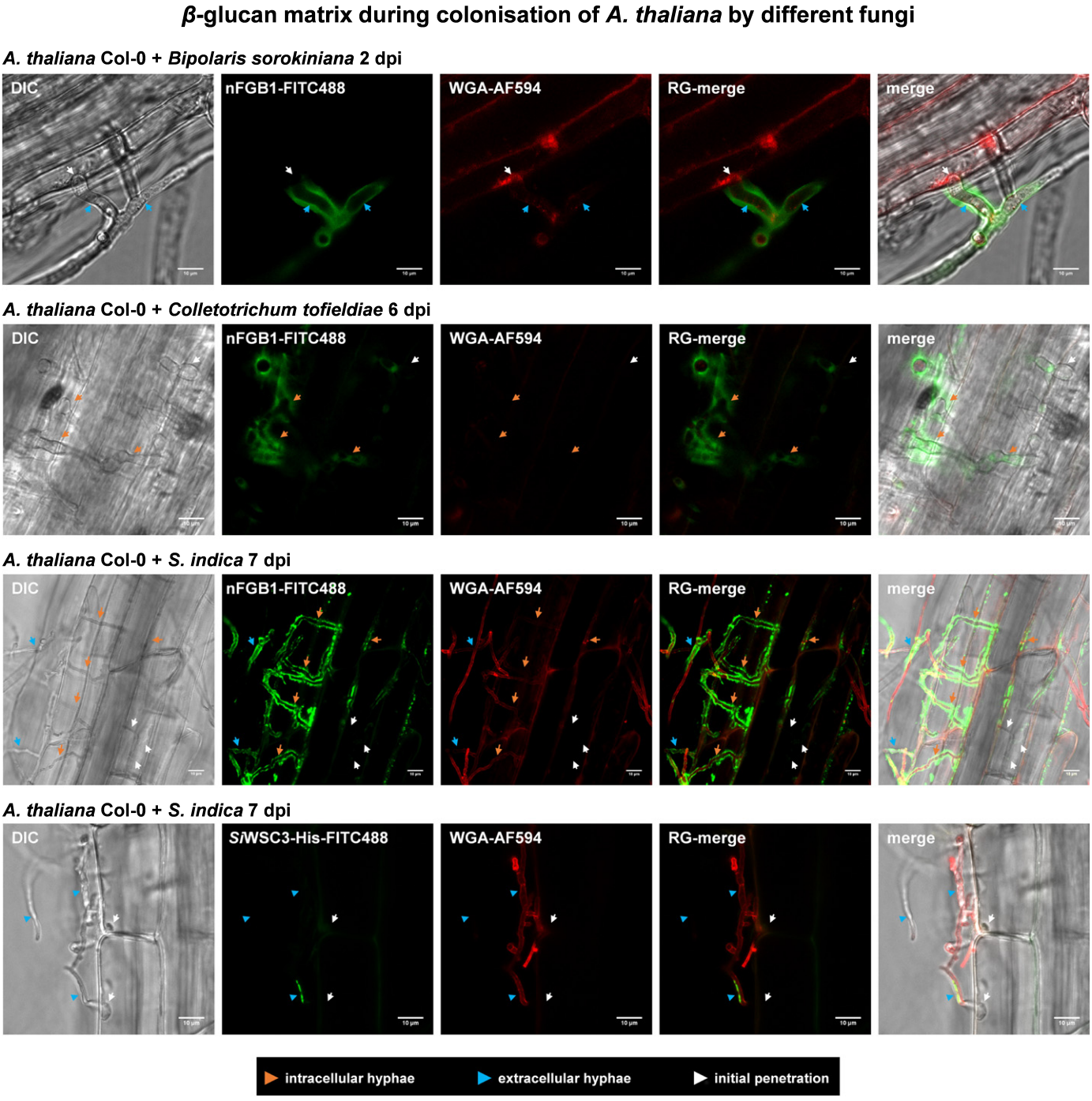

Fig. 5 Fungal extracellular β-glucan matrices in colonized *Arabidopsis thaliana* Col-0 roots. *Si*WSC3-His-FITC488 or nFGB1-FITC488 and WGA-AF594 were used to stain the following fungi *in planta*: *Bipolaris sorokiniana*, *Colletotrichum tofieldiae* and *Serendipita indica*. Samples were not fixed to maximize the preservation of exopolymeric material. Green fluorescence signal, FITC488 labeled nFGB1 or *Si*WSC3-His; red fluorescence signal, WGA-AF594; white arrows, initial penetration; blue arrows, extracellular hyphae; orange arrows, intracellular hyphae; dpi, d post-inoculation. Bars, 10 μm (see Supporting Information Fig. S8 for more details).

X. chrysenteron and cyanovirin-like lectin from *G. zeae*. Yet no relationship of these proteins to the infection process could be established (Birck *et al.*, 2004; Leonidas *et al.*, 2007; Koharudin *et al.*, 2011; Matei *et al.*, 2011; Skamnaki *et al.*, 2013; Varrot *et al.*, 2013). So far only lectins with LysM domains and *Si*FGB1 could be linked to plant colonization. A dual role was suggested for the chitin-binding LysM effectors ChELP1 and ChELP2 of the hemibiotrophic fungus *Colletotrichum higginsianum* and for *Si*FGB1 thus multiple functions might represent a common strategy of some fungal lectins (Takahara *et al.*, 2016). In our study the deregulation of *Si*FGB1 and *Si*WSC3 led to an alteration of fungal cell wall (CW) properties that is most clearly noticeable by the alteration of the response to CW stressors and by the binding of the β1-3-glucan antibody to the fungal CW (Figs 2g, S4c and

Wawra *et al.*, 2016). This indicates that both lectins are capable of interacting with the fungal CW. It was shown that during *S. indica* growth a large proportion of *Si*FGB1 is secreted into the culture supernatant (Wawra *et al.*, 2016) but no obvious accumulation of free *Si*WSC3 could be detected in this study. The absence of *Si*WSC3 in *S. indica* culture supernatant and the ability to agglutinate fungal cells hints to a potential role in strengthening the *S. indica* CW against external stresses and in adhesion between hyphal cells. The absence of an effect on colonization further supports the idea that this lectin does not have host immunosuppressive functions. Thus, we propose that *Si*WSC3 acts as a proteinaceous glue that connects neighboring β-glucan fibrils noncovalently in the CW of *S. indica*. Similar to the fungal Agglutinin-Like Sequence (Als) family, which includes sexual agglutinins, virulence factors and flocculins (Hoyer & Cota, 2016), the WSC lectin-like family could mediate cell–cell and cell–environment interactions.

Detection of β-glucans by lectins

Due to its remarkable strong binding affinity, specificity and small size, *Si*FGB1 represents a valuable tool to study CW development and composition in fungi and possibly also in oomycetes. The potential of *Si*FGB1 as a protein probe for β-glucans is exemplified by the labeling of the extracellular polysaccharide matrix with β1-6-linked glucoses surrounding fungal hyphae during root colonization. Such an extracellular matrix is known from bacteria and some fungal animal pathogens as polysaccharide cement crucial for the formation of biofilms and protection from the host enzymatic activity and recognition (Flemming & Wingender, 2010; Priegnitz *et al.*, 2012). The thick and diffuse appearance of the matrix in this study also is in line with results from a recent work where Kang and coworkers analyzed the CW architecture of the human pathogen *Aspergillus fumigatus* by solid-state nuclear magnetic resonance. There the authors found well-hydrated and relatively mobile matrix formed by β1-3, β1-4 and β1-6 linked glucans (Kang *et al.*, 2018).

Conclusions

Here we demonstrated that *Si*FGB1 requires β1-6-glucan linkages for efficient binding, whereas *Si*WSC3 binds indistinctly β1-6 branched and debranched long-chain β1-3-glucans. Direct comparison with the chemically labeled chitin-binding lectin wheat germ agglutinin (WGA) conjugated with the fluorescence dye Alexa Fluor 594 shows that *Si*FGB1 can be used to detect fungi not stainable with WGA-AF594. The existence of the two lectins *Si*WSC3 and *Si*FGB1 in *S. indica,* which both exhibit affinity to β-glucans but fulfill distinct biological tasks, illustrates the importance of β-glucan as an essential component of the fungal CW that needs to be fostered to prevent recognition while maintaining their integrity. Thus, the expansion for lectin WSC proteins in *S. indica* could enable this endophyte to cope with extremely challenging environments for the CW such as those found *in planta* and during confrontation with other fungi.

Acknowledgements

We thank Debika Sarkar for providing material for the *S. indica* – *B. sorokiniana* confrontation assay, Lisa Leson, Anna Wendel and Lucas Hüttebräucker for technical support. We acknowledge support from the Cluster of Excellence on Plant Science (CEPLAS, EXC 1028) and the Deutsche Forschungsgemeinschaft (DFG ZU 263/3-1 and ZU 263/2-1). J-HH was supported by the Deutsche Forschungsgemeinschaft (grant HE 7217/1-1) and by the Max Planck Society.

Author contributions

SW and PF performed the majority of the research; SW, PF, J-HH and AZ designed experiments and wrote the manuscript with input from the other coauthors; AZ supervised the project and acquired the funding; SW, HW and PF performed microscopy; TEM sample preparation and imaging was done by UN; bioinformatic analysis was carried out by UL and GL; and SB prepared debranched laminarin. SW and PF contibuted equally to this work.

ORCID

Jan-Hendrik Hehemann https://orcid.org/0000-0002-8700-2564
Gregor Langen https://orcid.org/0000-0002-8321-1756
Stephan Wawra https://orcid.org/0000-0001-8555-1618
Alga Zuccaro https://orcid.org/0000-0002-8026-0114

References

Andersson KM, Meerupati T, Levander F, Friman E, Ahren D, Tunlid A. 2013. Proteome of the nematode-trapping cells of the fungus *Monacrosporium haptotylum*. *Applied and Environmental Microbiology* **79**: 4993–5004.

Becker S, Scheffel A, Polz MF, Hehemann JH. 2017. Accurate quantification of laminarin in marine organic matter with enzymes from marine microbes. *Applied and Environment Microbiology* **83**. DOI: 10.1128/AEM.

Birck C, Damian L, Marty-Detraves C, Lougarre A, Schulze-Briese C, Koehl P, Fournier D, Paquereau L, Samama JP. 2004. A new lectin family with structure similarity to actinoporins revealed by the crystal structure of *Xerocomus chrysenteron* lectin XCL. *Journal of Molecular Biology* **344**: 1409–1420.

Bowman SM, Free SJ. 2006. The structure and synthesis of the fungal cell wall. *BioEssays* **28**: 799–808.

van den Burg HA, Harrison SJ, Joosten MHAJ, Vervoort J, de Wit PJGM. 2006. *Cladosporium fulvum* Avr4 protects fungal cell walls against hydrolysis by plant chitinases accumulating during infection. *Molecular Plant–Microbe Interactions* **19**: 1420–1430.

Chowdhury J, Henderson M, Schweizer P, Burton RA, Fincher GB, Little A. 2014. Differential accumulation of callose, arabinoxylan and cellulose in nonpenetrated versus penetrated papillae on leaves of barley infected with *Blumeria graminis* f. sp. *hordei*. *New Phytologist* **204**: 650–660.

Cohen-Kupiec R, Broglie KE, Friesem D, Broglie RM, Chet I. 1999. Molecular characterization of a novel beta-1,3-exoglucanase related to mycoparasitism of *Trichoderma harzianum*. *Gene* **226**: 147–154.

Dore J, Perraud M, Dieryckx C, Kohler A, Morin E, Henrissat B, Lindquist E, Zimmermann SD, Girard V, Kuo A *et al.* 2015. Comparative genomics, proteomics and transcriptomics give new insight into the exoproteome of the basidiomycete *Hebeloma cylindrosporum* and its involvement in ectomycorrhizal symbiosis. *New Phytologist* **208**: 1169–1187.

El Gueddari NE, Rauchhaus U, Moerschbacher BM, Deising HB. 2002. Developmentally regulated conversion of surface-exposed chitin to chitosan in cell walls of plant pathogenic fungi. *New Phytologist* **156**: 103–112.

Emsley P, Cowtan K. 2004. Coot: model-building tools for molecular graphics. *Acta Crystallographica. Section D, Biological Crystallography* **60**: 2126–2132.

Fesel PH, Zuccaro A. 2016a. beta-glucan: crucial component of the fungal cell wall and elusive MAMP in plants. *Fungal Genetics and Biology* **90**: 53–60.

Fesel PH, Zuccaro A. 2016b. Dissecting endophytic lifestyle along the parasitism/mutualism continuum in Arabidopsis. *Current Opinion in Microbiology* **32**: 103–112.

Finn RD, Mistry J, Tate J, Coggill P, Heger A, Pollington JE, Gavin OL, Gunasekaran P, Ceric G, Forslund K *et al.* 2010. The Pfam protein families database. *Nucleic Acids Research* **38**(Database issue): D211–D222.

Flemming HC, Wingender J. 2010. The biofilm matrix. *Nature Reviews Microbiology* **8**: 623–633.

Fujikawa T, Sakaguchi A, Nishizawa Y, Kouzai Y, Minami E, Yano S, Koga H, Meshi T, Nishimura M. 2012. Surface alpha-1,3-glucan facilitates fungal stealth infection by interfering with innate immunity in plants. *PLoS Pathogens* **8**: e1002882.

Futagami T, Nakao S, Kido Y, Oka T, Kajiwara Y, Takashita H, Omori T, Furukawa K, Goto M. 2011. Putative stress sensors WscA and WscB are involved in hypo-osmotic and acidic pH stress tolerance in *Aspergillus nidulans*. *Eukaryotic Cell* **10**: 1504–1515.

Gabius HJ, Andre S, Kaltner H, Siebert HC. 2002. The sugar code: functional lectinomics. *Biochimica Et Biophysica Acta-General Subjects* **1572**: 165–177.

Gaulin E, Jauneau A, Villalba F, Rickauer M, Esquerre-Tugaye MT, Bottin A. 2002. The CBEL glycoprotein of *Phytophthora parasitica* var. *nicotianae* is involved in cell wall deposition and adhesion to cellulosic substrates. *Journal of Cell Science* **115**: 4565–4575.

Geoghegan I, Steinberg G, Gurr S. 2017. The role of the fungal cell wall in the infection of plants. *Trends in Microbiology* **25**: 957–967.

Goldstein IJ, Hughes RC, Monsigny M, Osawa T, Sharon N. 1980. What should be called a lectin. *Nature* **285**: 66.

Guindon S, Dufayard JF, Lefort V, Anisimova M, Hordijk W, Gascuel O. 2010. New algorithms and methods to estimate maximum-likelihood phylogenies: assessing the performance of PhyML 3.0. *Systematic Biology* **59**: 307–321.

Herve C, Simeon A, Jam M, Cassin A, Johnson KL, Salmean AA, Willats WGT, Doblin MS, Bacic A, Kloareg B. 2016. Arabinogalactan proteins have deep roots in eukaryotes: identification of genes and epitopes in brown algae and their role in *Fucus serratus* embryo development. *New Phytologist* **209**: 1428–1441.

Hilbert M, Voll LM, Ding Y, Hofmann J, Sharma M, Zuccaro A. 2012. Indole derivative production by the root endophyte *Piriformospora indica* is not required for growth promotion but for biotrophic colonization of barley roots. *New Phytologist* **196**: 520–534.

Hiruma K, Gerlach N, Sacristan S, Nakano RT, Hacquard S, Kracher B, Neumann U, Ramirez D, Bucher M, O'Connell RJ *et al.* 2016. Root endophyte *Colletotrichum tofieldiae* confers plant fitness benefits that are phosphate status dependent. *Cell* **165**: 464–474.

Holmes KL, Lantz LM. 2001. Protein labeling with fluorescent probes. *Methods in Cell Biology* **63**: 185–204.

Hopke A, Brown AJP, Hall RA, Wheeler RT. 2018. Dynamic fungal cell wall architecture in stress adaptation and immune evasion. *Trends in Microbiology* **26**: 284–295.

Hoyer LL, Cota E. 2016. *Candida albicans* agglutinin-like sequence (Als) family vignettes: a review of Als protein structure and function. *Frontiers in Microbiology* **7**: 280.

de Jonge R, Thomma BPHJ. 2009. Fungal LysM effectors: extinguishers of host immunity? *Trends in Microbiology* **17**: 151–157.

de Jonge R, van Esse HP, Kombrink A, Shinya T, Desaki Y, Bours R, van der Krol S, Shibuya N, Joosten MHAJ, Thomma BPHJ. 2010. Conserved fungal LysM effector Ecp6 prevents chitin-triggered immunity in plants. *Science* **329**: 953–955.

Kamper J, Kahmann R, Bolker M, Ma LJ, Brefort T, Saville BJ, Banuett F, Kronstad JW, Gold SE, Muller O *et al.* 2006. Insights from the genome of the biotrophic fungal plant pathogen *Ustilago maydis*. *Nature* **444**: 97–101.

Kanagawa M, Satoh T, Ikeda A, Adachi Y, Ohno N, Yamaguchi Y. 2011. Structural insights into recognition of triple-helical beta-glucans by an insect fungal receptor. *Journal of Biological Chemistry* **286**: 29158–29165.

Kang X, Kirui A, Muszynski A, Widanage MCD, Chen A, Azadi P, Wang P, Mentink-Vigier F, Wang T. 2018. Molecular architecture of fungal cell walls revealed by solid-state NMR. *Nature Communications* **9**: 2747.

Kleemann J, Rincon-Rivera LJ, Takahara H, Neumann U, van Themaat EVL, van der Does HC, Hacquard S, Stuber K, Will I, Schmalenbach W *et al.* 2012. Sequential delivery of host-induced virulence effectors by appressoria and intracellular hyphae of the phytopathogen *Colletotrichum higginsianum*. *PLoS Pathogens* **8**: e1002643.

Koharudin LM, Viscomi AR, Montanini B, Kershaw MJ, Talbot NJ, Ottonello S, Gronenborn AM. 2011. Structure-function analysis of a CVNH-LysM lectin expressed during plant infection by the rice blast fungus *Magnaporthe oryzae*. *Structure* **19**: 662–674.

Kohler A, Kuo A, Nagy LG, Morin E, Barry KW, Buscot F, Canback B, Choi C, Cichocki N, Clum A *et al.* 2015. Convergent losses of decay mechanisms and rapid turnover of symbiosis genes in mycorrhizal mutualists. *Nature Genetics* **47**: 410–415.

Lahrmann U, Strehmel N, Langen G, Frerigmann H, Leson L, Ding Y, Scheel D, Herklotz S, Hilbert M, Zuccaro A. 2015. Mutualistic root endophytism is not associated with the reduction of saprotrophic traits and requires a noncompromised plant innate immunity. *New Phytologist* **207**: 841–857.

Lahrmann U, Zuccaro A. 2012. Opprimo ergo sum–evasion and suppression in the root endophytic fungus *Piriformospora indica*. *Molecular Plant–Microbe Interactions* **25**: 727–737.

Latge JP. 2007. The cell wall: a carbohydrate armour for the fungal cell. *Molecular Microbiology* **66**: 279–290.

Latge JP, Beauvais A, Chamilos G. 2017. The cell wall of the human fungal pathogen *Aspergillus fumigatus*: biosynthesis, organization, immune response, and virulence. *Annual Review of Microbiology* **71**: 99–116.

Leonidas DD, Swamy BM, Hatzopoulos GN, Gonchigar SJ, Chachadi VB, Inamdar SR, Zographos SE, Oikonomakos NG. 2007. Structural basis for the carbohydrate recognition of the *Sclerotium rolfsii* lectin. *Journal of Molecular Biology* **368**: 1145–1161.

Lodder AL, Lee TK, Ballester R. 1999. Characterization of the wsc1 protein, a putative receptor in the stress response of *Saccharomyces cerevisiae*. *Genetics* **152**: 1487–1499.

Maddi A, Dettman A, Fu C, Seiler S, Free SJ. 2012. WSC-1 and HAM-7 are MAK-1 MAP kinase pathway sensors required for cell wall integrity and hyphal fusion in *Neurospora crassa*. *PLoS ONE* **7**: e42374.

Marshall R, Kombrink A, Motteram J, Loza-Reyes E, Lucas J, Hammond-Kosack KE, Thomma BPHJ, Rudd JJ. 2011. Analysis of two *in planta* expressed LysM effector homologs from the fungus *Mycosphaerella graminicola* reveals novel functional properties and varying contributions to virulence on wheat. *Plant Physiology* **156**: 756–769.

Matei E, Louis JM, Jee J, Gronenborn AM. 2011. NMR solution structure of a cyanovirin homolog from wheat head blight fungus. *Proteins* **79**: 1538–1549.

Mayhew TM. 2011. Quantifying immunogold localization on electron microscopic thin sections: a compendium of new approaches for plant cell biologists. *Journal of Experimental Botany* **62**: 4101–4113.

Melida H, Sopena-Torres S, Bacete L, Garrido-Arandia M, Jorda L, Lopez G, Munoz-Barrios A, Pacios LF, Molina A. 2018. Non-branched-1,3-glucan oligosaccharides trigger immune responses in *Arabidopsis*. *The Plant Journal* **93**: 34–49.

Mentlak TA, Kombrink A, Shinya T, Ryder LS, Otomo I, Saitoh H, Terauchi R, Nishizawa Y, Shibuya N, Thomma BPHJ *et al.* 2012. Effector-mediated suppression of chitin-triggered immunity by *Magnaporthe oryzae* is necessary for rice blast disease. *Plant Cell* **24**: 322–335.

Micali CO, Neumann U, Grunewald D, Panstruga R, O'Connell R. 2011. Biogenesis of a specialized plant-fungal interface during host cell internalization of *Golovinomyces orontii* haustoria. *Cellular Microbiology* **13**: 210–226.

Mirelman D, Galun E, Sharon N, Lotan R. 1975. Inhibition of fungal growth by wheat-germ agglutinin. *Nature* **256**: 414–416.

Navarra G, Zihlmann P, Jakob RP, Stangier K, Preston RC, Rabbani S, Smiesko M, Wagner B, Maier T, Ernst B. 2017. Carbohydrate-lectin interactions: an unexpected contribution to affinity. *ChemBioChem* **18**: 539–544.

Oliveira-Garcia E, Deising HB. 2013. Infection structure-specific expression of beta-1,3-glucan synthase is essential for pathogenicity of *Colletotrichum graminicola* and evasion of beta-glucan-triggered immunity in maize. *Plant Cell* **25**: 2356–2378.

Oliveira-Garcia E, Deising HB. 2016. Attenuation of PAMP-triggered immunity in maize requires down-regulation of the key beta-1,6-glucan synthesis genes KRE5 and KRE6 in biotrophic hyphae of *Colletotrichum graminicola*. *The Plant Journal* **87**: 355–375.

Philip B, Levin DE. 2001. Wsc1 and Mid2 are cell surface sensors for cell wall integrity signaling that act through Rom2, a guanine nucleotide exchange factor for Rho1. *Molecular and Cellular Biology* **21**: 271–280.

Ponting CP, Hofmann K, Bork P. 1999. A latrophilin/CL-1-like GPS domain in polycystin-1. *Current Biology* **9**: R585–R588.

Priegnitz BE, Wargenau A, Brandt U, Rohde M, Dietrich S, Kwade A, Krull R, Fleissner A. 2012. The role of initial spore adhesion in pellet and biofilm formation in *Aspergillus niger*. *Fungal Genetics and Biology* **49**: 30–38.

Rajavel M, Philip B, Buehrer BM, Errede B, Levin DE. 1999. Mid2 is a putative sensor for cell integrity signaling in *Saccharomyces cerevisiae*. *Molecular and Cellular Biology* **19**: 3969–3976.

Rico-Ramirez AM, Roberson RW, Riquelme M. 2018. Imaging the secretory compartments involved in the intracellular traffic of CHS-4, a class IV chitin synthase, in *Neurospora crassa*. *Fungal Genetics and Biology* **117**: 30–42.

Rodicio R, Buchwald U, Schmitz HP, Heinisch JJ. 2008. Dissecting sensor functions in cell wall integrity signaling in *Kluyveromyces lactis*. *Fungal Genetics and Biology* **45**: 422–435.

Rovenich H, Zuccaro A, Thomma BP. 2016. Convergent evolution of filamentous microbes towards evasion of glycan-triggered immunity. *New Phytologist* **212**: 896–901.

Saloheimo M, Paloheimo M, Hakola S, Pere J, Swanson B, Nyyssonen E, Bhatia A, Ward M, Penttila M. 2002. Swollenin, a *Trichoderma reesei* protein with sequence similarity to the plant expansins, exhibits disruption activity on cellulosic materials. *European Journal of Biochemistry* **269**: 4202–4211.

Sanchez-Vallet A, Saleem-Batcha R, Kombrink A, Hansen G, Valkenburg DJ, Thomma BP, Mesters JR. 2013. Fungal effector Ecp6 outcompetes host immune receptor for chitin binding through intrachain LysM dimerization. *Elife* **2**: e00790.

Sawaguchi A, Ide S, Goto Y, Kawano J, Oinuma T, Suganuma T. 2001. A simple contrast enhancement by potassium permanganate oxidation for Lowicryl K4M ultrathin sections prepared by high pressure freezing/freeze substitution. *Journal of Microscopy* **201**: 77–83.

Schindelin J, Arganda-Carreras I, Frise E, Kaynig V, Longair M, Pietzsch T, Preibisch S, Rueden C, Saalfeld S, Schmid B *et al.* 2012. Fiji: an open-source platform for biological-image analysis. *Nature Methods* **9**: 676–682.

Skamnaki VT, Peumans WJ, Kantsadi AL, Cubeta MA, Plas K, Pakala S, Zographos SE, Smagghe G, Nierman WC, Van Damme EJ *et al.* 2013. Structural analysis of the *Rhizoctonia solani* agglutinin reveals a domain-swapping dimeric assembly. *Febs Journal* **280**: 1750–1763.

Sletmoen M, Stokke BT. 2008. Review: Higher order structure of (1,3)-beta-D-glucans and its influence on their biological activities and complexation abilities. *Biopolymers* **89**: 310–321.

Smith AJ, Graves B, Child R, Rice PJ, Ma ZC, Lowman DW, Ensley HE, Ryter KT, Evans JT, Williams DL. 2018. Immunoregulatory activity of the natural product laminarin varies widely as a result of its physical properties. *Journal of Immunology* **200**: 788–799.

Takahara H, Hacquard S, Kombrink A, Hughes HB, Halder V, Robin GP, Hiruma K, Neumann U, Shinya T, Kombrink E *et al.* 2016. *Colletotrichum higginsianum* extracellular LysM proteins play dual roles in appressorial function and suppression of chitin-triggered plant immunity. *New Phytologist* **211**: 1323–1337.

Tong SM, Chen Y, Zhu J, Ying SH, Feng MG. 2016. Subcellular localization of five singular WSC domain-containing proteins and their roles in *Beauveria bassiana* responses to stress cues and metal ions. *Environmental Microbiology Reports* **8**: 295–304.

Unfried F, Becker S, Robb CS, Hehemann J-H, Markert S, Heiden SE, Hinzke T, Becher D, Reintjes G, Krüger K *et al.* 2018. Adaptive mechanisms that provide competitive advantages to marine bacteroidetes during microalgal blooms. *ISME Journal* **12**: 2894–2906.

Varrot A, Basheer SM, Imberty A. 2013. Fungal lectins: structure, function and potential applications. *Current Opinion in Structural Biology* **23**: 678–685.

Verna J, Lodder A, Lee K, Vagts A, Ballester R. 1997. A family of genes required for maintenance of cell wall integrity and for the stress response in *Saccharomyces cerevisiae*. *Proceedings of the National Academy of Sciences, USA* **94**: 13804–13809.

Wawra S, Fesel P, Widmer H, Timm M, Seibel J, Leson L, Kesseler L, Nostadt R, Hilbert M, Langen G *et al.* 2016. The fungal-specific beta-glucan-binding lectin FGB1 alters cell-wall composition and suppresses glucan-triggered immunity in plants. *Nature Communications* 7. Doi: 10.1038/ncomms13188.

Zuccaro A, Lahrmann U, Guldener U, Langen G, Pfiffi S, Biedenkopf D, Wong P, Samans B, Grimm C, Basiewicz M *et al.* 2011. Endophytic life strategies decoded by genome and transcriptome analyses of the mutualistic root symbiont *Piriformospora indica*. *PLoS Pathogens* 7: e1002290.

Supporting Information

Additional Supporting Information may be found online in the Supporting Information section at the end of the article.

Fig. S1 Number of genes encoding putative lectins present in 79 fungal genomes.

Fig. S2 Phylogenetic relationships among proteins containing WSC domains.

Fig. S3 Sample numbers and raw data used for the relative quantification of chitin and β1-3-glucan.

Fig. S4 *Si*WSC3 increases cell wall stress resistance against Calcofluor White and Congo Red.

Fig. S5 *Si*WSC3 ligand binding analysis by CD spectroscopy and MST.

Fig. S6 Microscale thermophoresis raw data.

Fig. S7 *S. indica* spore viability and barley root colonization is not affected by *Si*WSC3.

Fig. S8 Microscopy images showing the presence of extracellular matrix in different root-associated fungi during colonization of *A. thaliana*.

Fig. S9 TEM example images of *S. indica* cells surrounded by a β-glucan matrix.

Methods S1 Supplemental materials and methods and primer list.

Table S1 List of functional protein domains involved in carbohydrate binding from 79 fungal genomes.

Please note: Wiley Blackwell are not responsible for the content or functionality of any Supporting Information supplied by the authors. Any queries (other than missing material) should be directed to the *New Phytologist* Central Office.